Supporting Information for

Triple-bridged helical binuclear copper(I) complexes. *Head-to-head* and *head-to-tail* isomerism and the solid-state luminescence

Aliia V. Shamsieva,*[a] Elvira I. Musina,[a] Tatiana P. Gerasimova,[a] Igor D. Strelnik,[a] Anna G. Strelnik,[a] Ilya E. Kolesnikov,[b] Alexey A. Kalinichev,[b] Daut R. Islamov,[a] Aida I. Samigullina,[a] Peter Lönnecke,[c] Sergey A. Katsyuba,[a] Evamarie Hey-Hawkins,[c] Andrey A. Karasik[a], Oleg G. Sinyashin[a]

[a] *Arbuzov Institute of Organic and Physical Chemistry, FRC Kazan Scientific Center, Russian Academy of Sciences, Arbuzov Street 8, 420088 Kazan, Russian Federation*
[b] *Center for Optical and Laser Materials research, Research Park of St. Petersburg State University, Ulianovskaya Street 5, 198504 St. Petersburg, Russian Federation*
[c] *Institut für Anorganische Chemie der Universität Leipzig, 29 Johannisallee, 04103 Leipzig, Germany*

Contents

Table S1. The crystallographic data for single crystals of **1**HH, **2**HH, **2**HT, **3**HT, **4**HT.

Compound	**1**HH	**2**HT	**2**HH	**3**HT	**4**HT
Method of crystallization	The crystals were grown from chloroform/ethanol mother liquor of **1**HH	The crystals were grown by slow evaporation of chloroform solution of **2**HH	The crystals were grown by slow evaporation of an ethanol mother liquor of **2**HH	The crystals were grown by vapor diffusion of diethyl ether into a dichloromethane solution of **3**HH	The crystals were grown by vapor diffusion of diethyl ether into a dichloromethane solution of **4**HH
Molecular formula	$C_{27}H_{36}Cu_2Br_{0.18}Cl_{0.82}N_3P_3^+ (Cl^-) \times 3H_2O]$	$C_{27}H_{36}BrCu_2N_3P_3^+ (Br^-) \times 2EtOH$	$C_{27}H_{36}BrCu_2N_3P_3^{1+} Br^{1-}$	$C_{27}H_{36}Cu_2N_3P_3^{2+} 2(BF_4^-)$	$C_{30}H_{42}Cu_2N_3P_3^{2+}\ 2(BF_4^{1-}) \times CH_2Cl_2$
Empirical formula	$C_{27}H_{42}BrCl_2Cu_2N_3O_3P_3$	$C_{31}H_{48}Br_2Cu_2N_3O_2P_3$	$C_{27}H_{36}Br_2Cu_2N_3P_3$	$C_{27}H_{36}Cu_2N_3P_3B_2F_8$	$C_{31}H_{44}Cu_2N_3P_3B_4F_8Cl_2$
Formula weight	755.53	874.53	782.40	796.20	923.20
Temperature [K]	130(2)	170(2)	100(2)	150(2)	100(2)
Wavelength	0.71073 Å	0.71073 Å	0.71073 Å	0.71073 Å	0.71073 Å
Crystal system	Trigonal	Triclinic	Monoclinic	Triclinic	Monoclinic
Space group	$P\bar{3}c1$ (No. 165)	$P\bar{1}$ (No. 2)	$C2/c$ (No. 15)	$P\bar{1}$ (No. 2)	$P2_1/n$ (No. 14)
Unit cell dimensions					
a [Å]	1429.57(2)	922.70(5)	25.0528(18)	10.1721(5)	14.598(2)
b [Å]	1429.57(2)	1407.96(6)	13.4498(10)	12.2241(6)	17.269(2)
c [Å]	1788.33(2)	1466.01(5)	18.7389(13)	14.7284(7)	31.380(4)
α [deg]	90	84.174(3)		90.611(1)	
β [deg]	90	78.867(4)	94.492(3)	103.374(1)	100.502(6)
γ [deg]	120	76.930(4)		99.224(1)	
Volume [Å^3]	3165.1(1)	1816.94(15)	6294.8(8)	1756.52(15)	7778.2(17)
Z	4	2	8	2	8
$\rho_{(calculated)}$ [g/cm^3]	1.586	1.599	1.651	1.505	1.577
μ [mm^{-1}]	1.910	3.533	4.065	1.413	1.421
F(000)	1557	888	3136	808	3760
Crystal size [mm^3]	0.30 x 0.15 x 0.10	0.25 x 0.20 x 0.05	0.534 × 0.268 × 0.25	0.272 × 0.141 × 0.123	0.458 × 0.318 × 0.312
Θ_{Min} - Θ_{Max} [deg]	2.278 to 32.560	1.992 to 32.635	2.002 to 25.805	1.423 to 30.063	1.320 to 25.383
Index ranges	$-21 \le h \le 21, -21 \le k \le 20, -27 \le l \le 26$	$-13 \le h \le 13, -21 \le k \le 21, -21 \le l \le 1$	$-30 \le h \le 30, -16 \le k \le 16, -22 \le l \le 22$	$-14 \le h \le 14, -17 \le k \le 17, -20 \le l \le 20$	$-17 \le h \le 17, -20 \le k \le 20, -36 \le l \le 37$

Reflections collected	41937	27187	46204	79742	63265
Indp. reflections [R_{int}]	3716 [0.0413]	11896 [0.0326]	6020 [0.0663]	10279 [0.0395]	14194 [0.1141]
Completeness [Θ_{Max}]	100% (30.510°)	100% (30.510°)	99.6% (25.242°)	100% (25.242°)	99.9% (25.242°)
T_{Max} / T_{Min}	1.00000 / 0.90525	1.00000 / 0.79607	0.1752 / 0.0882	0.7543 / 0.6877	0.5072 / 0.4140
Restraints / parameters	21 / 136	84 / 427	293 / 418	37 / 416	556 / 1082
Gof on F^2	1.026	1.023	1.651	1.031	1.085
R_1 / wR_2 ($I>2\sigma(I)$)	0.0449 / 0.1165	0.0426 / 0.0932	0.0569 / 0.1551	0.0293 / 0.0660	0.0612 / 0.1414
R_1 / wR_2 (all data)	0.0714 / 0.1304	0.0712 / 0.1069	0.0736 / 0.1661	0.0428 / 0.0705	0.1178 / 0.1758
Residual electron density [$e \cdot Å^{-3}$]	0.549 and -1.086	1.262 and -0.977	1.852 and –0.811	0.568 and –0.415	1.180 and –1.249
CCDC No	2003271	20032712	2000253	2000251	2000252

Comments on the structure of 1HH*$[Cu_2Br_{0.18}Cl_{0.82}(C_9H_{12}NP)_3][(Cl)(H_2O)_3$**:** Structure solution with SHELXT-2014 (Dual-space method). Anisotropic refinement of all non-hydrogen atoms, except disordered atoms C(7'), C(8'), Cl(2) and O(2), with SHELXL-2018. All hydrogen atoms were calculated on idealized positions. The PC_4H_8-ring is disordered with a ratio of 0.77(1):0.23(1). The complex was synthesized from CuCl (> 99 purity) without bromo containing solvents or reagents. However, assuming a Cl(1) / Br(1) disorder (ratio 0.819(4) : 0.181(4)), the final structure parameters could be improved. The molecular formulae of the compound may be given as $[Cu_2Br_{0.18}Cl_{0.82}(C_9H_{12}NP)_3]$ $[(Cl)(H_2O)_3]$ (Fig. S1). Water molecules (O2) and the chloride anions (Cl2) are disordered within the $[(H_2O)_6Cl_2]$-cube (Fig. S2). Hydrogen atoms of this water-chloride-cube are only calculated for illustration and are disordered as well, e. g. the hydrogen atom H1O1 of O1 can only once interact with an adjacent O1' atom. This hydrogen disorder was disregarded.

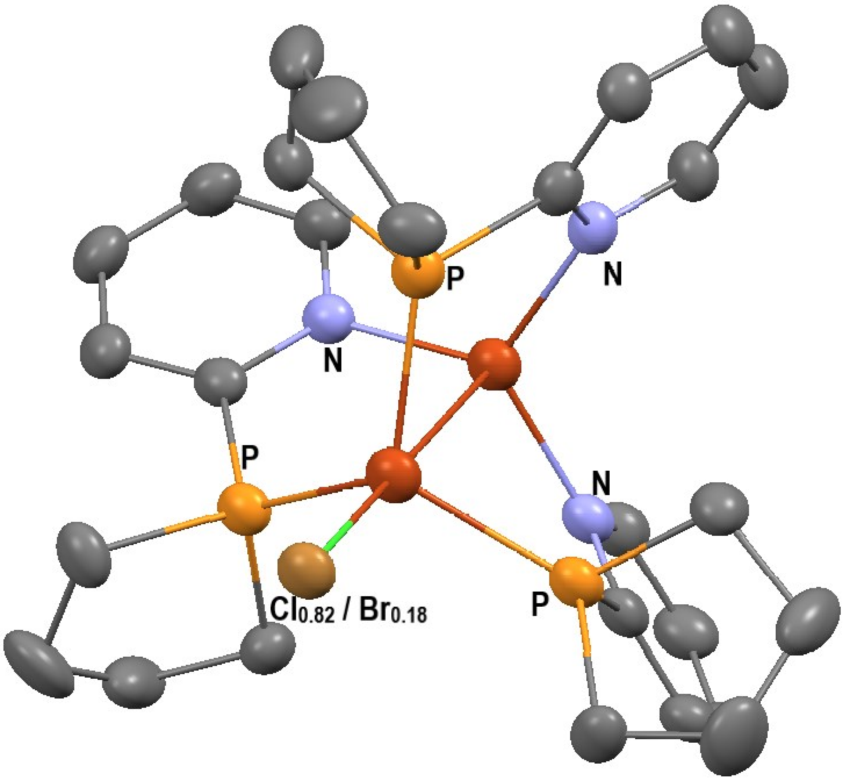

Figure S1. Monocation of **1**HH*[$Cu_2Br_{0.18}Cl_{0.82}(C_9H_{12}NP)_3$]. Hydrogen atoms are omitted for clarity.

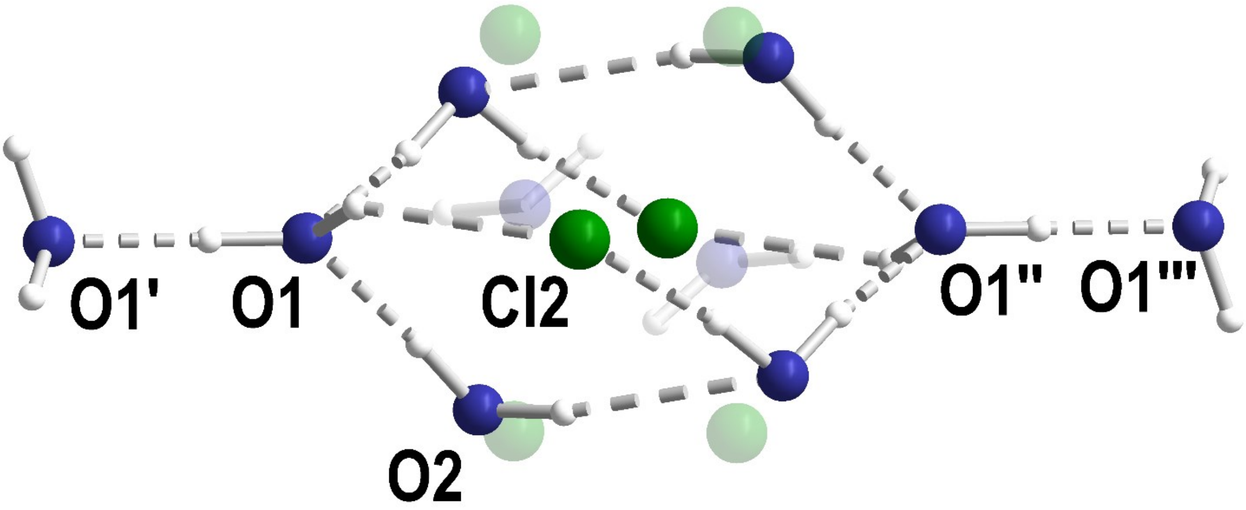

Figure S2. Disordered water-cationic chain of **1**HH on the threefold c-axis with calculated hydrogen donor acceptor bonds for one possible arrangement (Disordered non-hydrogen atoms are given in transparent mode). The "water-chloride-cube" is located on a special position (Wyckoff letter b with the site symmetry $\bar{3}\ .\ .$) whereas O1 and O1' are related by twofold rotation (Wyckoff letter a with the site symmetry $3\ 2\ .$).

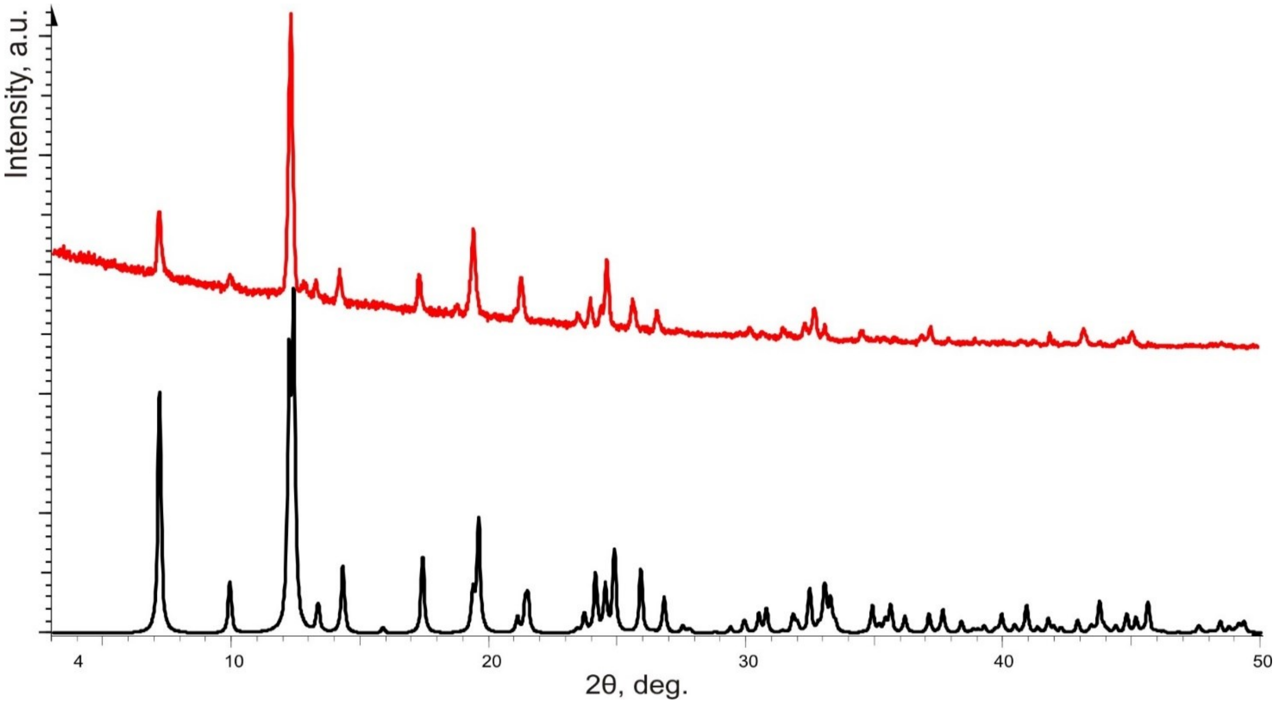

Figure S3. The theoretical powder diffractogram (black line) calculated from single X-ray data for compound **1**HH and the experimental powder diffractograms of polycrystalline powder sample (red line).

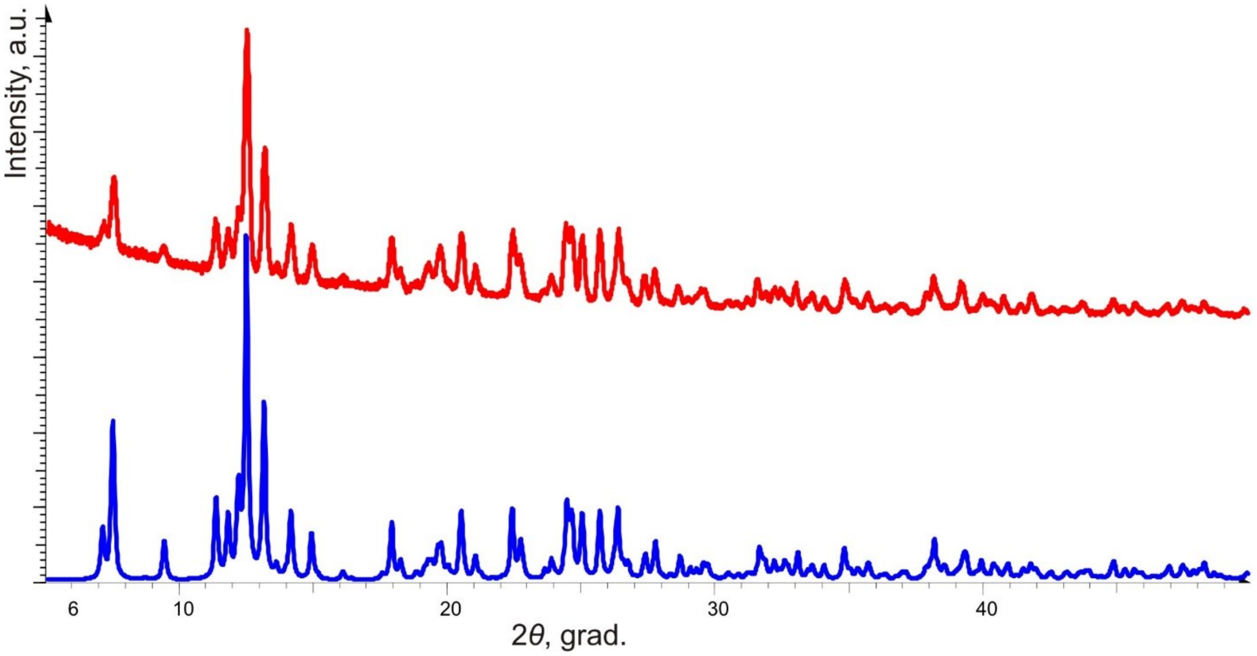

Figure S4. The theoretical powder diffractogram (blue line) calculated from single X-ray data for compound **2**HH and the experimental powder diffractograms of polycrystalline powder sample (red line).

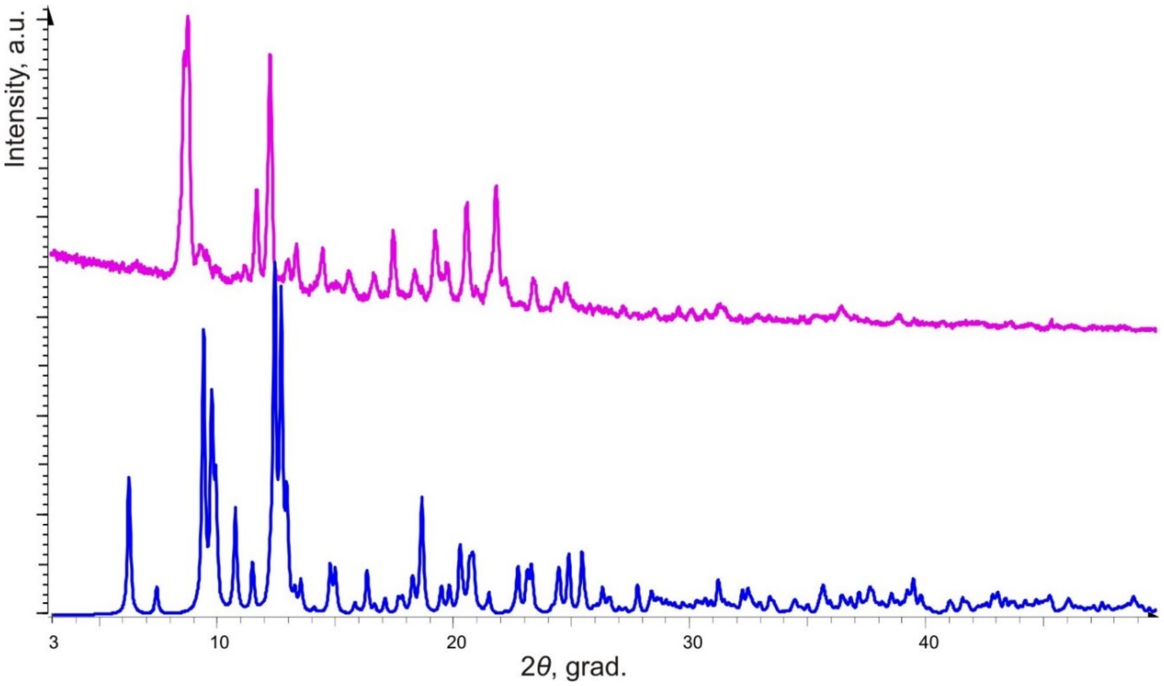

Figure S5. The theoretical powder diffractogram (blue line) calculated from single X-ray data for compound **3**HT and the experimental powder diffractograms of polycrystalline powder sample (violet line).

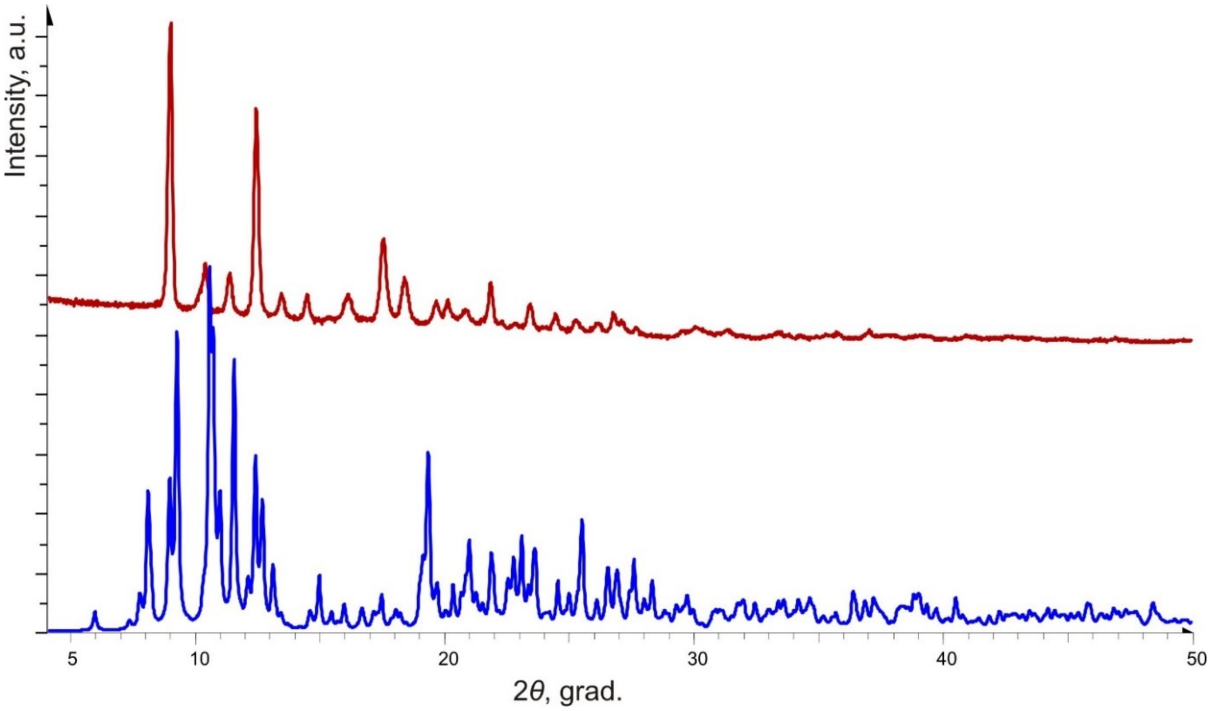

Figure S6. The theoretical powder diffractogram (blue line) calculated from single X-ray data for compound **4**HT and the experimental powder diffractograms of polycrystalline powder sample (brown line).

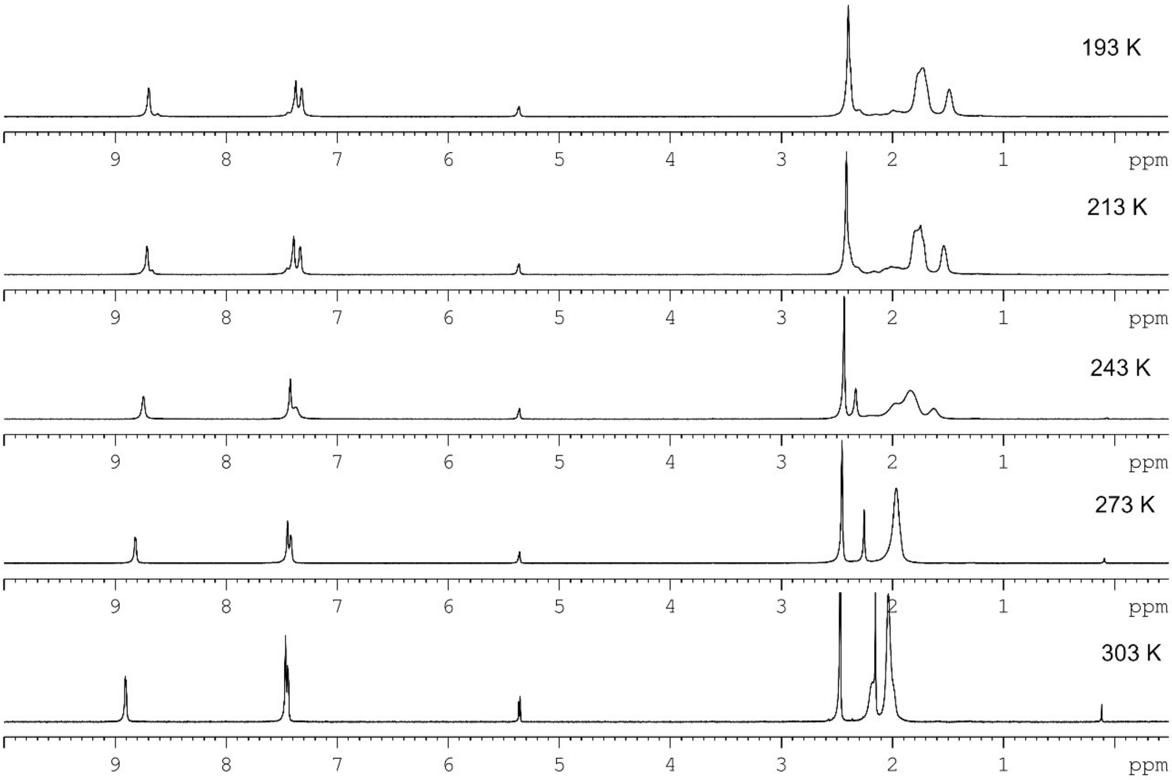

Figure S7. The variable-temperature ^{1}H NMR spectra of **4** in CD_2Cl_2.

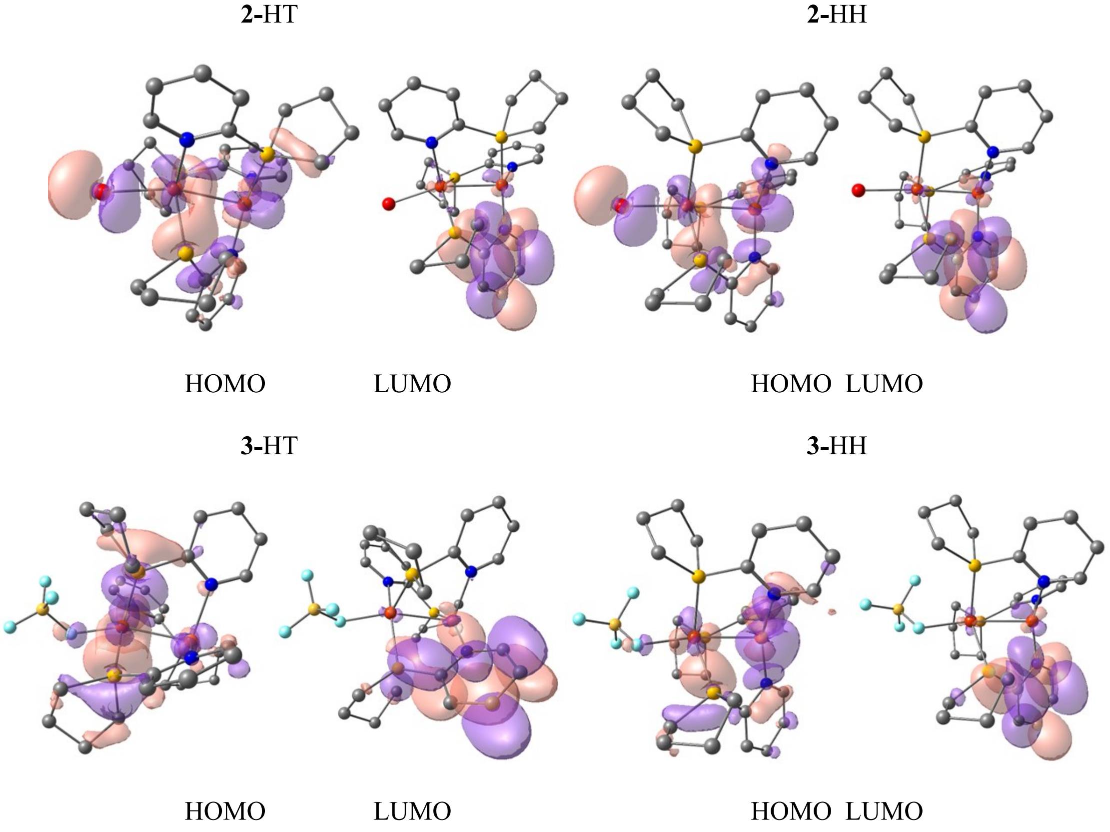

2-HT

2-HH

HOMO LUMO

HOMO LUMO

3-HT

3-HH

HOMO LUMO

HOMO LUMO

Figure S8. HOMOs and LUMOs of S_0 states of HH and HT isomers of **2** and **3**, calculated on the optimized T_1 structures.

Table S2. Calculated excitation energies (nm), oscillator strengths (f), and assignments of the electronic transitions of **2**HH.

λ, nm	f	assignment	Plots of frontier orbitals, mostly contributing the transition	
337	0.004	HOMO->LUMO	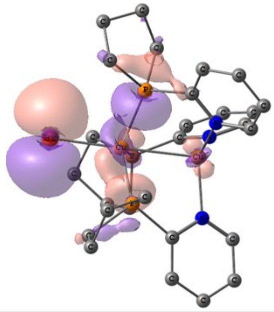	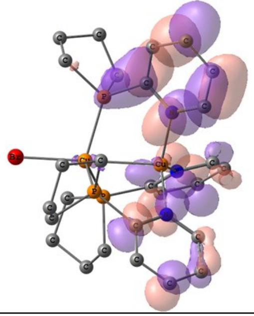
333	0.003	mixed		
331	0.006	HOMO^{-1}->LUMO^{+1}	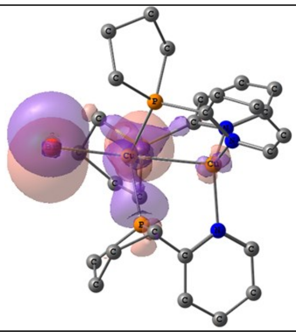	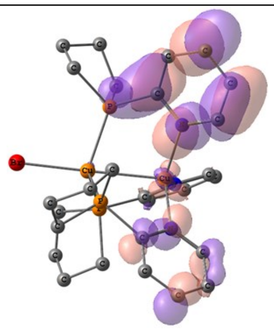
320	0.002	mixed		
319	0.001	mixed		
316	0.002	mixed		
310	0.007	HOMO^{-2}->LUMO	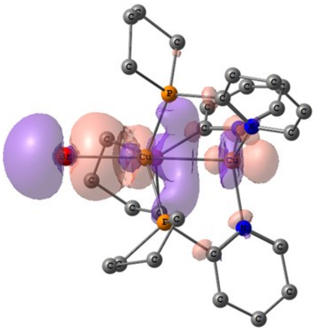	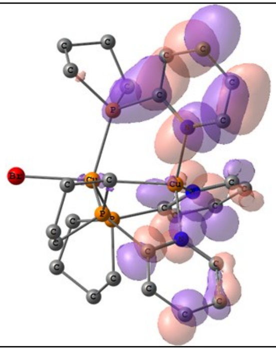
309	0.000	HOMO^{-2}->LUMO^{+2}		
308	0.016	HOMO^{-1}->LUMO^{+1}	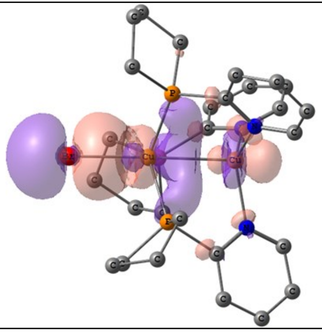	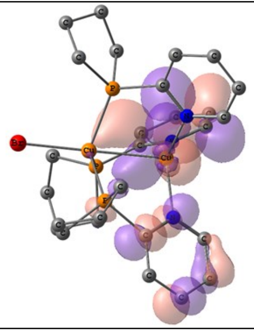

Table S3. Calculated excitation energies (nm), oscillator strengths (f), and assignments of the electronic transitions of **2**HT.

λ, nm	f	assignment	Plots of frontier orbitals, mostly contributing the transition	
330	0.035	HOMO->LUMO	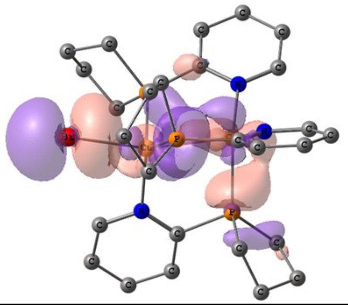	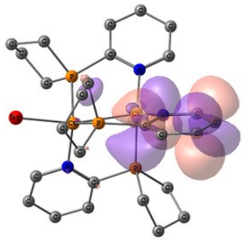
326	0.008	HOMO->LUMO^{+1}	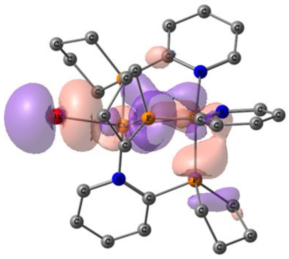	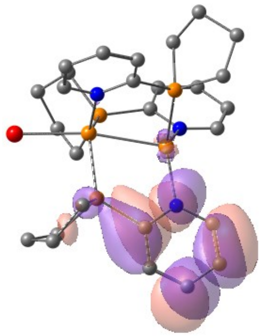
319	0.008	HOMO->LUMO^{+2}	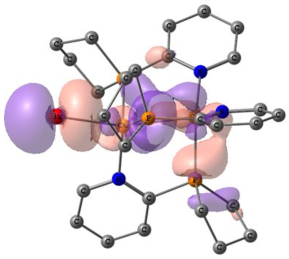	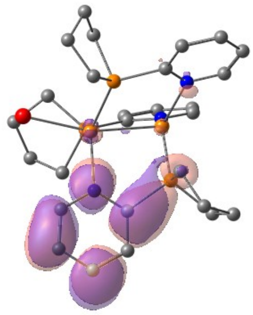
304	0.007	mixed		
300	0.037	HOMO^{-1}->LUMO^{+2}	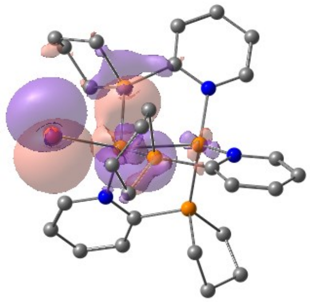	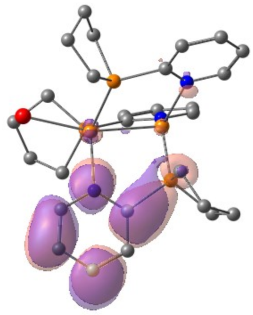
298	0.011	mixed		
296	0.010	HOMO->LUMO^{+3}	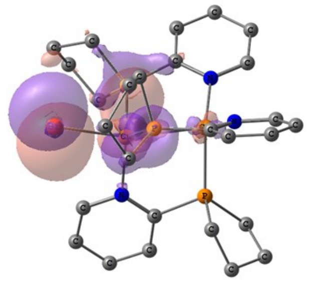	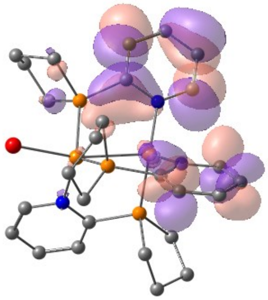

Table S4. Calculated excitation energies (nm), oscillator strengths (f), and assignments of the electronic transitions of **3**HH.

λ, nm	f	assignment	Plots of frontier orbitals, mostly contributing the transition	
323	0.001	HOMO->LUMO	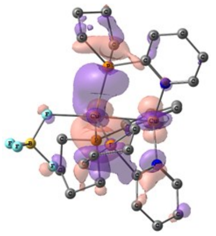	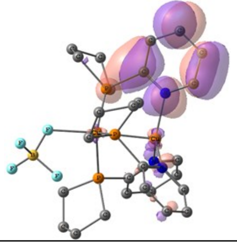
317	0.0041	HOMO^{-4}->LUMO	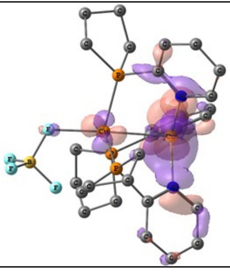	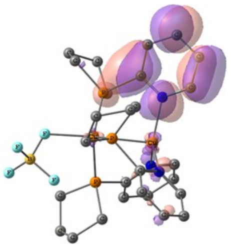
311	0.0046	HOMO->LUMO HOMO->LUMO^{+1}	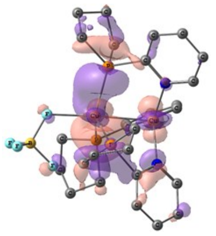	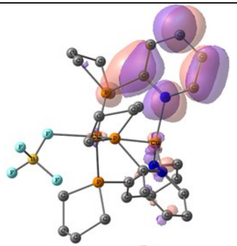 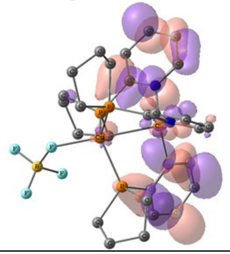
310	0.0038	HOMO^{-3}->LUMO^{+2}	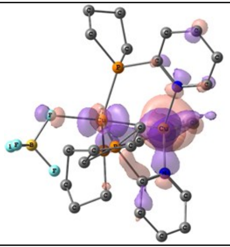	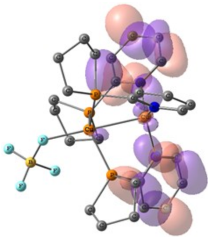
305	0.0018	HOMO^{-1}->LUMO^{+1}	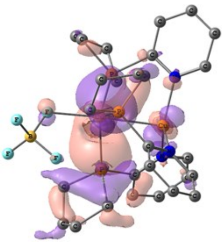	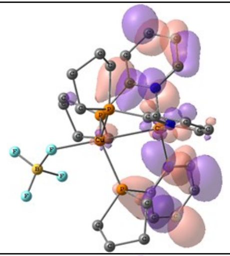
296	0.0132	HOMO^{-3}->LUMO^{+1}	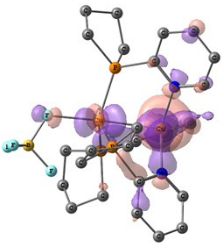	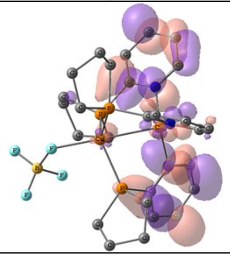

292	0.0771	HOMO^{-2}->LUMO^{+2}	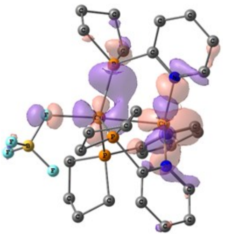	
288	0.0279	HOMO^{-3}->LUMO^{+2}		
285	0.0719	HOMO^{-4}->LUMO^{+3}		
280	0.0158	HOMO^{-3}->LUMO^{+4}		
279	0.0182	HOMO^{-2}->LUMO^{+1} HOMO^{-3}->LUMO^{+1}	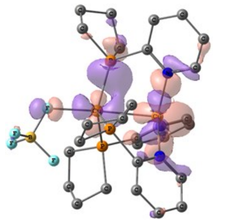	

Table S5. Calculated excitation energies (nm), oscillator strengths (f), and assignments of the electronic transitions of **3**HT.

λ, nm	f	assignment	Plots of frontier orbitals, mostly contributing the transition	
325	0.0097	HOMO->LUMO	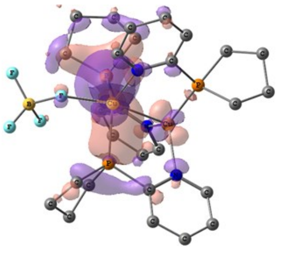	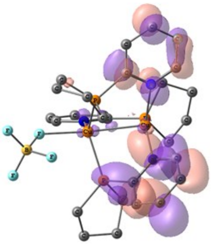
304	0.0539	HOMO^{-1}->LUMO	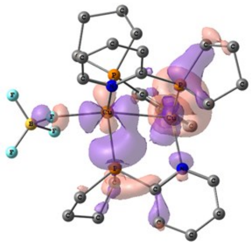	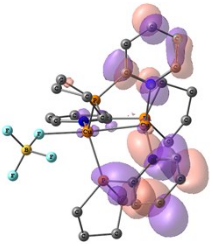
300	0.0229	HOMO->LUMO^{+1}	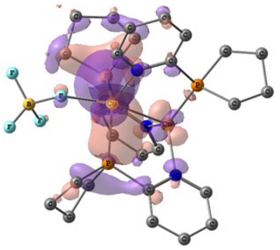	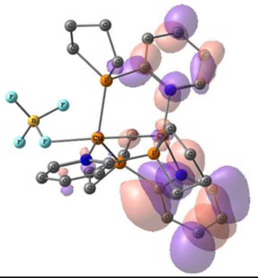
299	0.0302	HOMO->LUMO^{+2}	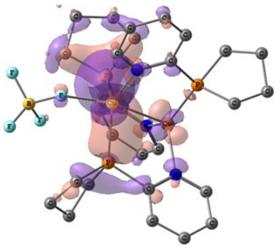	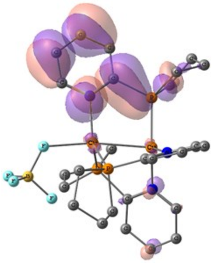
290	0.017	HOMO^{-1}->LUMO^{+1}	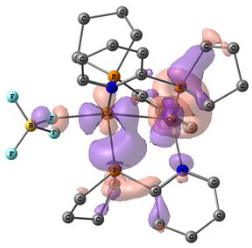	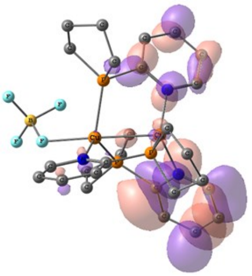
286	0.0045	mixed		
275	0.0074	mixed		
275	0.0107	HOMO^{-4}->LUMO	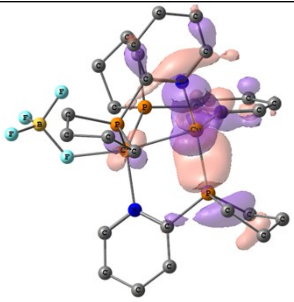	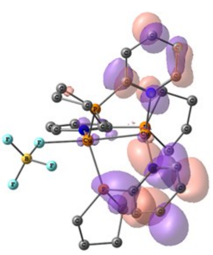

273	0.0141	HOMO^{-2}->LUMO^{+2}	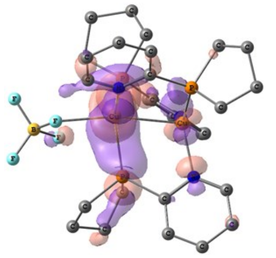	

Table S6. Selected structural parameters predicted for S$_0$ and T$_1$ optimized geometries of **2**HT, **2**HH, **3**HT, **3**HH.

	2HT		**2**HH		**3**HT		**3**HT	
	S$_0$	T$_1$	S$_0$	T$_1$	S$_0$	T$_1$	S$_0$	T$_1$
dCu-Cu, Å	2.60	2.52	2.61	2.56	2.57	2.59	2.61	2.49
dCu-Br/ dCu-F, Å	2.45	2.39	2.41	2.44	2.19	2.09	2.13	2.08
dCu-N, Å	2.04	1.91	2.05	1.88	2.04	1.94	2.05	1.88
dCu-P, Å	2.29	2.29	2.28	2.31	2.30	2.30	2.30	2.31
dN-C, Å	1.34	1.40	1.35	1.41	1.35	1.39	1.35	1.41
dC-P, Å	1.85	1.78	1.85	1.80	1.85	1.78	1.85	1.79
N-Cu-Cu-P, º	5	45	27	48	-6	-34	36	48
N-Cu-N/ N-Cu-P, º	129	153	119	152	137	153	125	151
Cu-Cu-Br/ Cu-Cu-F, º	163	157	177	176	169	160	177	165

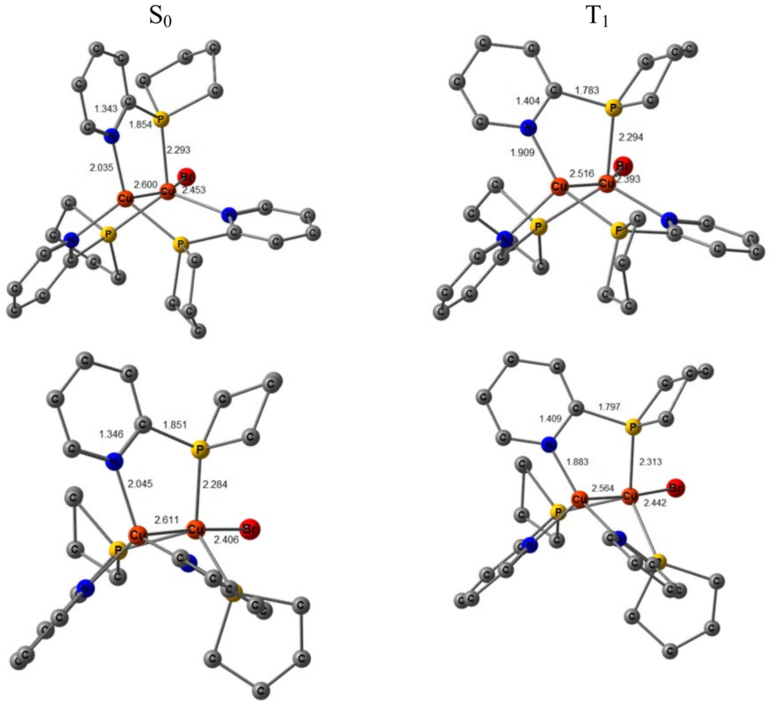

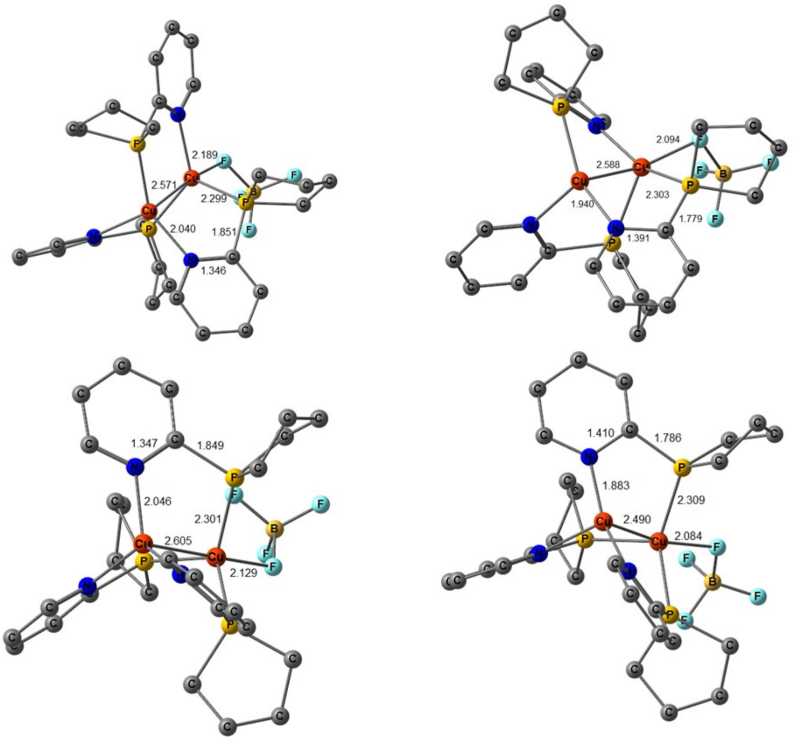

Figure S9. Optimized structures and predicted bond lengths for S_0 and T_1 states of **2**HT, **2**HH, **3**HT, **3**HH.

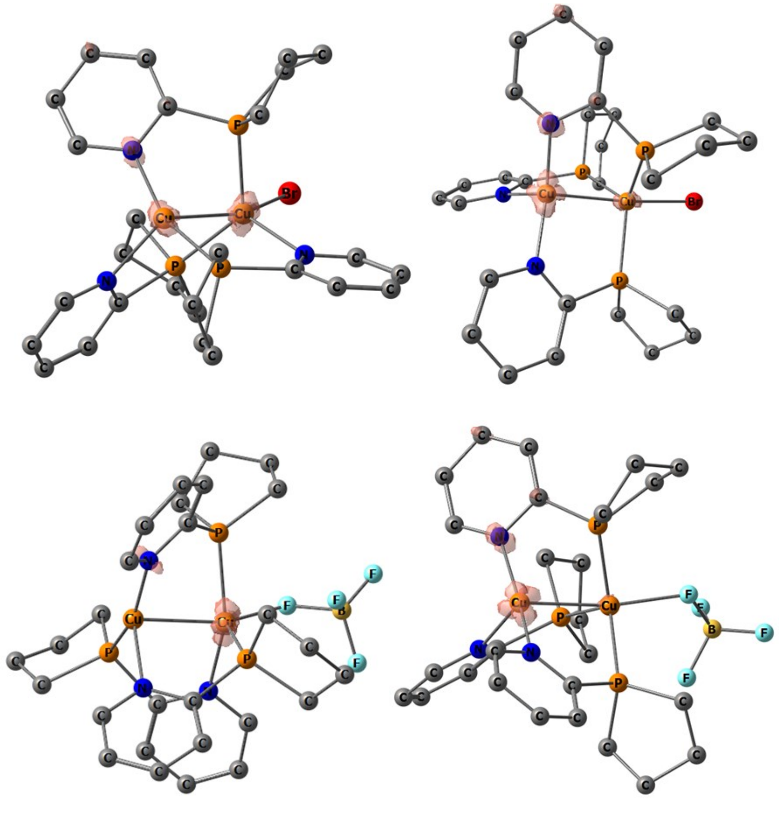

Figure S10. Plot of spin density calculated for T_1 optimized geometries of **2**HT, **2**HH, **3**HT, **3**HH.